Volume 10, Issue 3, 2020, 5455 - 5459 ISSN 2069-5837
Biointerface Research in Applied Chemistry
www.BiointerfaceResearch.com
https://doi.org/10.33263/BRIAC103.455459
Original Research Article Open Access Journal
Received: 21.01.2020 / Revised: 03.03.2020 / Accepted: 06.03.2020 / Published on-line: 09.03.2020

Magnetic properties of Cu and Al doped nano $BaFe_{12}O_{19}$ ceramics

G. Packiaraj [1], Mohd. Hashim [2], K. Chandra Babu Naidu [3], G. Helen Ruth Joice [4], J. Laxman Naik [5], D. Ravinder [6], B. Ramakrishna Rao [7]

[1]Department of Physics, Aditya College of Engineering, Surampalem, Kakinada – 533437, Andhra Pradesh, India
[2]Department of Applied Physics, Aligarh Muslim University, Aligarh 202002, India
[3]Department of Physics, GITAM Deemed to be University, Bangalore-562163, India
[4]Assistant Professor of Physics, ThiruKollanjiappar Arts College,Vriddhachalam-606001, Cuddalore Dist., Tamilnadu, India
[5]Department of Physics, University College of Science, Saifabad, Hyderabad- 500004, Osmania University, Telangana, India
[6]Department of Physics, Osmania University, Hyderabad-500007, Telangana, India
[7]Department of Chemistry, GITAM Deemed to be University, Bangalore-562163, Karnataka, India
*corresponding author e-mail address: ***ravindergupta28@rediffmail.com*** | Scopus ID 57190787725

ABSTRACT

The $BaCu_xFe_{12-x}O_{19}$ and $BaAl_xFe_{12-x}O_{19}$ (x = 0.0, 0.4, 0.8, 1.2) materials were prepared via sol-gel auto combustion technique. Further, the X-ray diffraction patterns suggested the formation of single phase hexagonal structure. This work is aimed to study the effect of diamagnetic and paramagnetic elements on magnetic characteristics of $BaFe_{12}O_{19}$. The results established that in the case of diamagnetic (Cu) substitution, the saturation magnetization was increased and decreased alternatively. Furthermore, it was noticed that the coercivity values of all doped samples were lower than those of undoped samples. But the replacement of Fe^{3+} with paramagnetic (Al) element led to a decrease in saturation magnetization and to a significant increase in the coercive field.

Keywords:*Hexaferrites; Magnetism; Sol-Gel; Magnetic Properties.*

1. INTRODUCTION

M-type hexaferrite, the composition of which is represented by $MeFe_{12}O_{19}$ (Me = Ba, Sr or Pb) belongs to a class of ferrimagnetism [1]. It has various applications in the form of permanent magnets, microwave absorber, high density magnetic recording media, transformer core, magnetic fluids for biological applications, etc [1]. The crystalline structure of the hexagonal ferrites is the result of close packing of oxygen ion layers. The divalent and trivalent metallic cations are located in interstitial sites of the structure; while the heavy Ba or Sr ions enter substitutionaly the oxygen layers [2]. By replacing the cation and composition with suitable elements, one can prepare different types of ferrites with significant magnetic and electric characteristics. In the literature, it was observed that the effect of ferroelectric cations like Ba, Sr and Pb on the ferrites, hexaferrites and perovskite systems was elucidated in order to study the structural, electrical, optical, magnetic, piezo electric, magnetocaloric and ferroelectric properties [3 - 18]. These cations may replace the iron or titanium sites depending upon the preferable site occupation. Moreover, it was observed that the above mentioned properties were changed in a significant way. However, in this study we concentrated on replacing Fe^{3+} ion by other less magnetic moment, paramagnetic or diamagnetic cations can affect the exchange interactions between the magnetic sublattices, which further alter the high uniaxial anisotropy field of the barium hexaferrites [3]. Especially, these Ba and Al cations can influence the magnetic properties of hexaferrites also. However, it is known that the electrical, optical and magnetic properties of ferrites are very sensitive to the particle sizes, shape and degree of crystallinity. At present, tremendous efforts have been made to achieve highly homogeneous nano-particles of barium hexaferrite by using different synthesis methods [4]. Among all synthesis methods, Sol-gel combustion techniques show advantages mainly due to low cost, ability to produce multi-component oxides with single phase and invariably in the nanometer range. In present work, Series of 'Cu' doped $BaCu_xFe_{12-x}O_{19}$ and 'Al' doped $BaAl_xFe_{12-x}O_{19}$ (x = 0.0, 0.4, 0.8, 1.2) hexaferrites have been prepared separately using sol-gel auto combustion technique. The effects of diamagnetic and paramagnetic elements on structural and magnetic characteristics of $BaFe_{12}O_{19}$ were investigated.

2. MATERIALS AND METHODS

Experimental procedure.

Both divalent and trivalent substituted M-type hexaferrites $BaCu_xFe_{12-x}O_{19}$ and $BaAl_xFe_{12-x}O_{19}$ have been prepared using Sol-gel auto combustion technique separately. Corresponding metal nitrates, citric acid and aqueous ammonia solution were used as raw materials. Initially, stoichiometric amount of metal nitrates and citric acid were dissolved in double distilled water with help of magnetic stirrer attached with hot plate. The solution was neutralized by adding ammonia solution drop by drop and the neutralized solution was maintained at 80°C for the continuous evaporation. Finally, the solution was changed into a viscous gel and self ignited to form ash eruption. The combusted powder was crushed and calcined at 500°C followed by 950°C for 4 hour. The obtained samples were characterized byanalyzing the structure and magnetic properties. In view of this, the diffraction study was carried out using XRD (Bruker). Field-dependent magnetization measurements of prepared samples were carried out at room temperature using a VSM (EG & G Princeton Applied Research; Model 4500). A small amount of sample was tightly filled in a non-magnetic plastic tube and mounted on the VSM sample

holder. Thereafter, hysteresis curve was recorded under a maximum field of ±15 kOe.

3. RESULTS

The X-ray diffraction patterns of copper and aluminium doped barium hexaferrites were presented in Fig.1 & 2 respectively. It was observed from Fig.1 that all the peaks were of good crystallinity in nature. The increase of Cu-content from 0.0 to 1.2 enhanced the intensity of crystalline phases. In addition, the diffraction peaks were compared with the standard JCPDS: 27 – 1029 of $BaFe_{12}O_{19}$. It was noticed that all the diffraction planes were in good consistent with the hexagonal phases of $BaFe_{12}O_{19}$. Thus, it was confirmed that the resultant structure of compound was remained constant (hexagonal) upon doping the copper element. The average crystallite size (D) was computed using Scherrer formula mentioned in references [19 - 24]. The results showed that the 'D' was varying between 34 to 72 nm unsystematically as a function of Cu-content. This was attributed to the unsystematic variation of microstrain which could be developed during the reaction process. Similar observations were reported in the literature [25-27]. In the same way, the diffraction patterns of Al doped $BaFe_{12}O_{19}$ was depicted in Fig.2. Herein, it was identified that the intensity of diffraction phases was diminished upon increasing the Al content. In addition, it became constant at high Al contents. The reflection planes were similar to the reflection planes of $BaFe_{12}O_{19}$. The 'D' values were observed to be altering from 24 to 69 nm as a function of Al content in $BaFe_{12}O_{19}$ system.

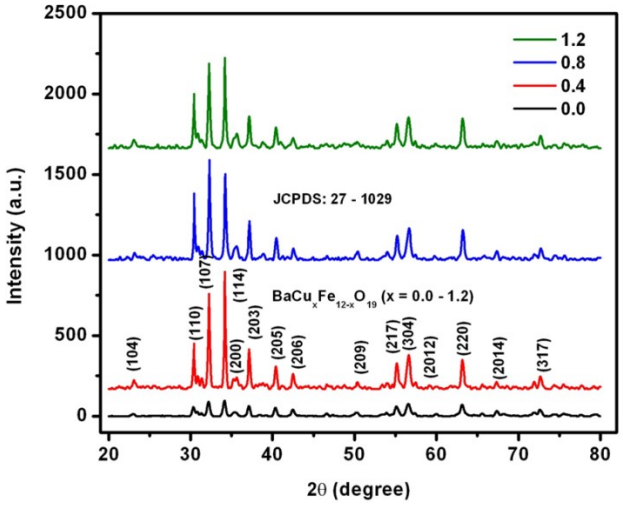

Figure 1. XRD spectra of Cu substituted barium hexaferrite samples.

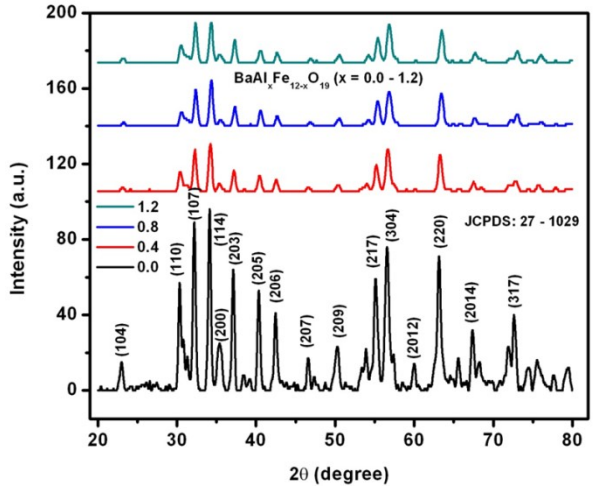

Figure 2. XRD spectra of Al substituted barium hexaferrite samples.

Generally, magnetic strength of M-type hexaferrite depend on 12 Fe^{3+} ions distributed over five distinct sites i.e. 2a, 2b, 4f1, 4f2 and 12k. Out of these five, 2a, 4f2 and 12k are octahedral, 4f1 is tetrahedral and the last 2b is trigonal bipyramid. The 12 Fe^{3+} are arranged as 6 Fe^{3+} are in 12k site having the spin up, 2 ions in 4f2 and 4f1 having spin down and 1 ion in 2a and 2b site having to spin up. So the 8 Fe^{3+} are in the upward direction and 4 in the downward direction. So 4 upward spin and downward spin cancel each other and the net magnetic moment is obtained of 4 Fe^{3+}per formula units. According to the configuration of Fe^{3+}, there are 5 unpaired electrons in the 3d orbital, each Fe^{3+}ion has the magnetic moment of 5μB and the total moment is 20 μB per formula unit [28, 29]. Fig. 3 shows hysteresis loops of $BaCu_xFe_{12-x}O_{19}$ (x = 0.0, 0.4, 0.8, 1.2) hexaferrite samples. Magnetic parameters such as saturation magnetization (M_s), coercivity (H_c)and remanent magnetization (M_r) were calculated and listed in Table 1. The variation of the saturation magnetization, coercivityand remanent magnetizationas a function of Cu concentration are shown in Fig. 4.

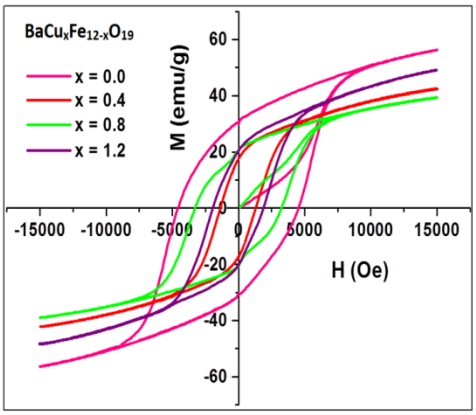

Figure 3. Hysteresis loops of Cu substituted barium hexaferrite samples.

Table 1. Magnetic parameters of Cu substituted barium hexaferrites.

Samples	M_s(emu/g)	M_r(emu/g)	M_r / M_s	H_c (Oe)
$BaFe_{12}O_{19}$	56.24	30.00	0.533	4625
$BaCu_{0.4}Fe_{11.6}O_{19}$	41.2	18.1	0.439	1422
$BaCu_{0.8}Fe_{11.2}O_{19}$	39.30	20.70	0.527	3250
$BaCu_{1.2}Fe_{10.8}O_{19}$	48.1	21.0	0.437	1918

The saturation magnetization was decreased with the addition of copper content till x = 0.8 and raised for the sample x = 1.2. The variation of M_s can be explained on the basis of microstructure and distribution of cations at different sites in the crystal structure of hexaferrite [30]. Initially, the low values of M_s with the increase of Cu^{2+} content may be due to the occupancy of ions at 2b sites [31]. Usually, large size and non-magnetic dopant ions prefer to occupy octahedral sites [32]. Since ionic radius of Cu^{2+} is larger than that of Fe^{3+}, maximum number of Cu ion may prefer the octahedral sites (2a, 4f2 and 12k), which enhances the hyperfine fields and strengthening the Fe^{3+} – O – Fe^{3+} super-exchange interaction giving higher net magnetization, therefore the value of M_s reaches to 48.1 emu/g for x = 1.2 sample [33]. Copper substitution in barium hexaferrite led to a significant decrease of H_c compared to that of pure $BaFe_{12}O_{19}$hexaferrite. The value of coercivity in barium hexaferrite is attributed to its high uniaxial anisotropy along the c-axis. The decrease in H_c can be

related to the reduction of the anisotropy field in the presence of Cu^{2+} ions. Saturation magnetization also plays a direct role in decreasing coercivity through Brown's relation [34] which is given by

$$H_c \geq 2k_1/\mu' M_s \quad (1)$$

Where, μ' is the initial permeability and k_1 anisotropy energy. According to this relation, H_c is inversely proportional to M_s. In the copper substituted composition, the sample with x = 0.8 shows least saturation magnetization and highest coercivity. The variation in H_c can also be due to the existence of grain boundary as defects during magnetization process [31].The measured hysteresis loops for the Al substituted $BaAl_xFe_{12-x}O_{19}$(x = 0.0, 0.4, 0.8, 1.2) hexaferrite samples as a function of the applied magnetic field are shown in Fig. 5 and the magnetic parameters are listed in Table 2. An increase in the coercivity from 4625 Oe to 7375 Oe and decrease in the saturation magnetization and remanence magnetization from 56.24 to 19.18 emu/g and from 30.0 to 11.55 emu/g, respectively were observed for the Al-substituted barium ferrite. The increase in coercivity and decrease in the magnetizations with Al substitution is in agreement with the observation made for Al-substituted barium hexaferrite prepared by the conventional ceramic method [30].

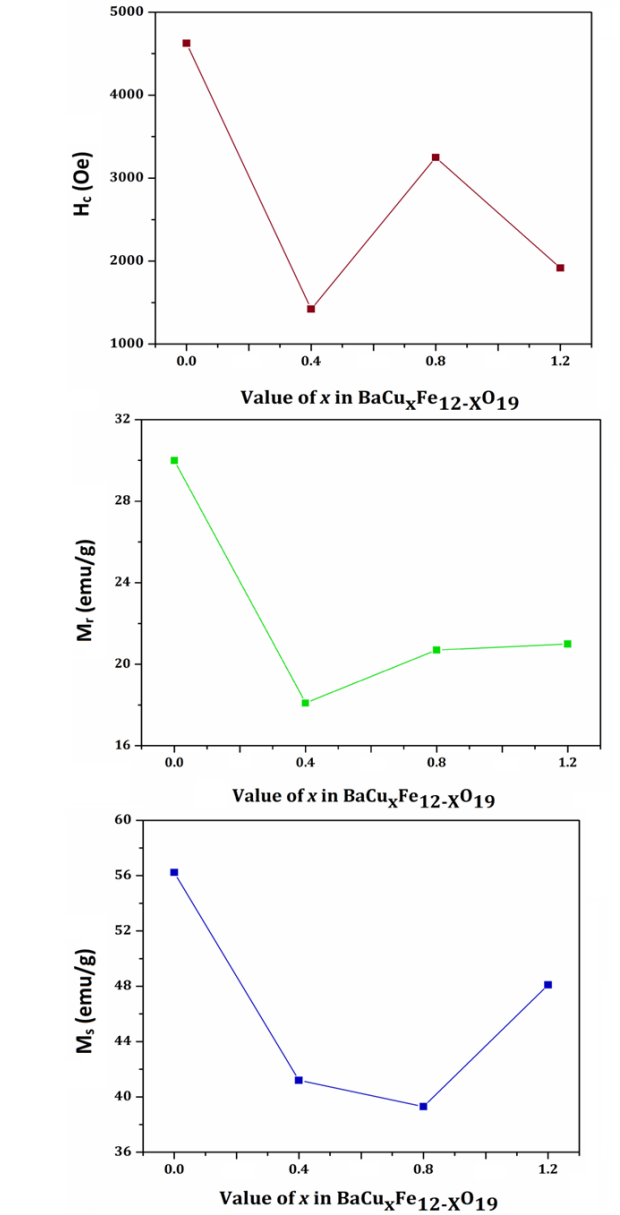

Figure 4. Variations of magnetic parameters with copper concentration.

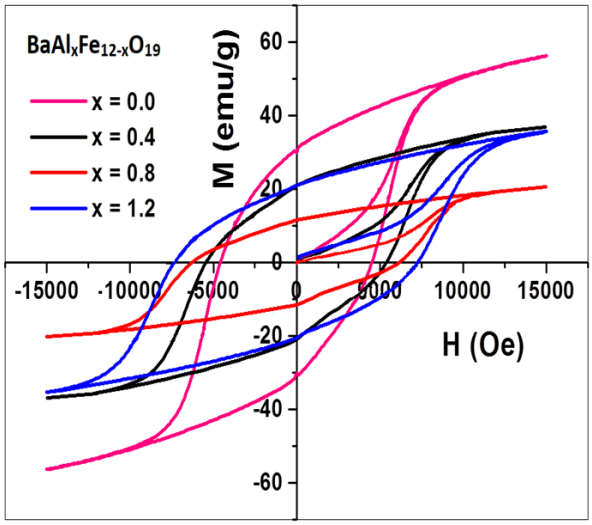

Figure 5. Hysteresis loops of Al substituted barium hexaferrite samples.

Table 2. Magnetic parameters of Al substituted barium hexaferrites.

Samples	M_s(emu/g)	M_r(emu/g)	M_r / M_s	H_c (Oe)
$BaAl_{0.4}Fe_{11.6}O_{19}$	37.52	21.07	0.562	5500
$BaAl_{0.8}Fe_{11.2}O_{19}$	19.18	11.55	0.602	6500
$BaAl_{1.2}Fe_{10.8}O_{19}$	35.69	21.02	0.589	7375

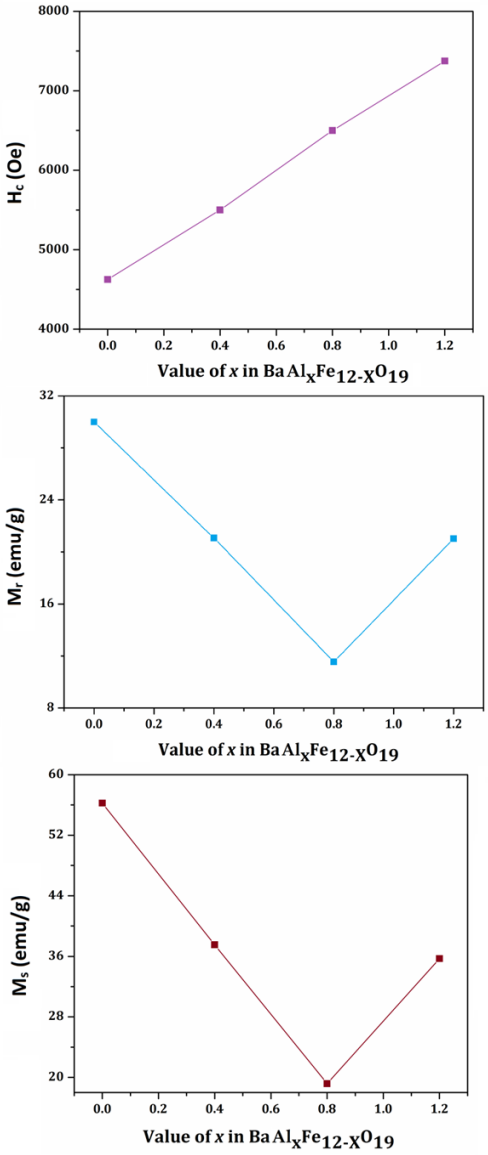

Figure 6. Variations of magnetic parameters with Aluminium concentration.

Uncompensated upward spins of Fe^{3+} ions in the lattice sites play a vital role inthe net magnetic moment in M-type

hexaferrite composition. In the present study, Fe^{3+} ions with magnetic moment of 5 μB are replaced by Al^{3+} ions with zero magnetic moment. So the inability of Al^{3+} ions to cancel out spin down moments of Fe^{3+} ions leads to the reduction in saturation magnetization and remanence of the substituted samples (Fig. 6). Also diamagnetic nature of Al reduces the super-exchange interaction between Fe^{3+}- O - Fe^{3+} and causes a non-collinear spin arrangement [35]. The sample $BaAl_{1.2}Fe_{10.8}O_{19}$ (x = 1.2) shows different behaviour, it has a little higher value of saturation and remanence magnetization compared the sample with x = 0.8. It may be the effect of lattice defects and amorphous aluminium oxide created in the combustion process [36]. The coercivity increases with an increase in Aluminium concentration; this may be attributed to the increase in anisotropy field H_a and decrease in the saturation magnetization.

Moreover, it was observed that the squareness of x = 0.0 – 1.2 contents of Cu doped barium hexaferrites revealed the values altering from 0.437 – 0.533 (Table.1). These values are < 0.5 (M_r/M_s< 0.5) for x = 0.4 and 1.2 contents. In case of x = 0.0 and 0.8 contents, the squareness was above 0.5. Similarly, the Al doped barium hexaferrites offered the squareness value more than 0.5 for all x = 0.0 – 1.2 contents. However, it was a reported fact that if the squareness is greater than 0.5 ($M_r/M_s\geq$ 0.5), the materials contain larger number of single magnetic domain while the same materials will have multi-magnetic domains in the case of squareness is less than 0.5 ($M_r/M_s\leq$ 0.5) [35, 36]. Hence, this confirmed a fact that the x = 0.4 & 1.2 contents of $BaCu_xFe_{12-x}O_{19}$ samples showed the multi-domain magnetic structure while the rest of the contents ensured the single domain magnetic structure.

On the other hand, the $BaAl_xFe_{12-x}O_{19}$ (x = 0.0, 0.4, 0.8, 1.2) material compositions showed the complete single-magnetic domain nature due to having the M_r/M_s values greater than 0.5. As a whole, it was identified that the doping of Cu into the barium hexaferrite system exhibited the mixed domain structure while the Al doping into the barium hexaferrite system provided the single domain magnetic structure.

4. CONCLUSIONS

The Cu and Al doped M-type barium hexaferrite with chemical composition $BaCu_xFe_{12-x}O_{19}$ and $BaAl_xFe_{12-x}O_{19}$ (x = 0.0, 0.4, 0.8, 1.2) were successfully synthesized via sol-gel auto combustion technique. The hexagonal structure of samples remained the same upon doping the copper and aluminium into the barium hexaferrite system. Replacement of Fe^{3+} with different size and nonmagnetic Cu^{2+} and Al^{3+} ions reduced the super exchange interaction and alter the collinear spin alignments. These led to the random variation of saturation and remanence magnetization in substituted samples. Variations in the coercivity values are reversed with the substitution of diamagnetic and paramagnetic elements. The net coercivity decreased with Cu substitution and increased with Al substitution. Hence, the present study gives platform to understand and tailor the magnetic characteristics of barium hexaferrite upon doping Cu and Al elements.

5. REFERENCES

1. Asiri, S.; Güner, S.; Demir, A.; Yildiz, A.; Manikandan, A.; Baykal, A. Synthesis and Magnetic Characterization of Cu Substituted Barium Hexaferrites. *Journal of Inorganic and Organometallic Polymers and Materials* **2018**, *28*, 1065-1071, https://doi.org/10.1007/s10904-017-0735-1.
2. Goldman, A. *Modern Ferrite Technology.* Springer publication, 2006.
3. Raghuram, N.; Rao, T.S.; Babu Naidu, K.C. Investigations on functional properties of hydrothermally synthesized Ba1-xSrxFe12O19 (x = 0.0 − 0.8) nanoparticles. *Materials Science in Semiconductor Processing* **2019**, *94*, 136-150, https://doi.org/10.1016/j.mssp.2019.01.037.
4. Tasleem, M.; Hashim, M.; Naidu, K.C.B.; Ali, S.A.; Ravinder, D. Optical and electronic properties of copper and cobalt substituted nano SrBaFe12O19 synthesized by sol–gel autocombustion method. *Applied Physics A* **2019**, *125*, https://doi.org/10.1007/s00339-019-2618-5.
5. Naidu, K.; Reddy, V.; Sarmash, S.; Doraiswamy, K.; Subbarao, T.; Nagasamudram, S.K. Structural, morphological, electrical, impedance and ferroelectric properties of BaO-ZnO-TiO2 ternary system. *Journal of the Australian Ceramic Society* **2018**, *55*, https://doi.org/10.1007/s41779-018-0225-0.
6. Kumar, N.S.; Suvarna, R.P.; Babu Naidu, K.C. Sol-gel synthesized and microwave heated Pb0.8-yLayCo0.2TiO3 (y = 0.2–0.8) nanoparticles: Structural, morphological and dielectric properties. *Ceramics International* **2018**, *44*, 18189-18199, https://doi.org/10.1016/j.ceramint.2018.07.027.
7. Doraiswamy, K. Structural, morphological and optical properties of Ba1-xCuxTiO3 (X = 0.2, 0.4, 0.6, 0.8) nanoparticles synthesizedby hydrothermal method. *Materials Chemistry and Physics* **2018**.
8. Suresh Kumar, N.; Padma Suvarna, R.; Chandra Babu Naidu, K. Structural and ferroelectric properties of microwave heated lead cobalt titanate nanoparticles synthesized by sol–gel technique. *Journal of Materials Science: Materials in Electronics* **2018**, *29*, 4738-4742, https://doi.org/10.1007/s10854-017-8429-6.
9. Ram, N.R.; Prakash, M.; Naresh, U.; Kumar, N.S.; Sarmash, T.S.; Subbarao, T.; Kumar, R.J.; Kumar, G.R.; Naidu, K.C.B. Review on Magnetocaloric Effect and Materials. *Journal of Superconductivity and Novel Magnetism* **2018**, *31*, 1971-1979, https://doi.org/10.1007/s10948-018-4666-z.
10. Prakash M.; Jeevan Kumar R.; Chandra Babu Naidu K.;, Optical and functional properties of hydrothermally synthesized tetragonal $Ba_{0.4}Cu_{0.6-x}La_xTiO_3$ (x=0.2–0.6) nanoparticles. *Mater. Res. Express* **2020**, *7*, 015037, https://doi.org/10.1088/2053-1591/ab6494
11. Kumar, N.S.; Suvarna, R.P.; Naidu, K.C.B. Multiferroic Nature of Microwave-Processed and Sol-Gel Synthesized NanoPb1-xCoxTiO3 (x = 0.2–0.8) Ceramics. *Crystal Research and Technology* **2018**, *53*, 1800139, https://doi.org/10.1002/crat.201800139.
12. Kumar, N.S.; Suvarna, R.P.; Naidu, K.C.B. Multiferroic Nature of Microwave-Processed and Sol-Gel Synthesized NanoPb1-xCoxTiO3 (x = 0.2–0.8) Ceramics. *Crystal Research and Technology* **2018**, *53*, https://doi.org/10.1002/crat.201800139.
13. Kothandan, D.; Jeevan Kumar, R.; Chandra Babu Naidu, K. Barium titanate microspheres by low temperature hydrothermal method: studies on structural, morphological, and optical properties. *Journal of Asian Ceramic Societies* **2018**, *6*, 1-6, https://doi.org/10.1080/21870764.2018.1439607.

14. Reddy, V.; Sarmash, S.; Chandra Babu Naidu, K.; Maddaiah, M.; Subbarao, T. Structural and optical properties of BaO-ZnO-TiO2 ternary system. *Journal of Ovonic Research* **2016**, *12*, 261-266.
15. Kumar, N.; Suvarna, R.; Chandra,B.N.K.; Singampalli, R.; Srinivas, K.; Basha, B. Optical bandgap and ferroelectric studies of Pb 0.8− y La y Co 0.2 TiO 3 (y = 0.2 to 0.8) synthesized by microwave irradiation processed sol-gel technique. *Advances in Natural Sciences: Nanoscience and Nanotechnology* **2019**, *10*.Dastagiri S.; Lakshmaiah M. V.; Chandra Babu Naidu K.; Defect dipole polarization mechanism in low-dimensional Europium substituted $Al_{0.8}La_{0.2}TiO_3$ nanostructures. *Physica E: Low-dimensional Systems and Nanostructures* **2020**, *120*, 114058, https://doi.org/10.1016/j.physe.2020.114058
16. Chandra. B.N.K. Optical, Magnetic and Ferroelectric Properties of Ba0.2Cu0.8-xLaxFe2O4 (x = 0.2 - 0.6) Nanoparticles. *Ceramics International* **2019**.
17. Naresh, U.; Kumar, R.J.; Naidu, K.C.B. Hydrothermal synthesis of barium copper ferrite nanoparticles: Nanofiber formation, optical, and magnetic properties. *Materials Chemistry and Physics* **2019**, *236*, https://doi.org/10.1016/j.matchemphys.2019.121807.
18. Cullity, B.D. *Elements of X-ray diffraction*. 2nd ed. Addison-Wesley, Reading, MA, 1978.
19. Boda, N.; Boda, G.; Naidu, K.C.B.; Srinivas, M.; Batoo, K.M.; Ravinder, D.; Reddy, A.P. Effect of rare earth elements on low temperature magnetic properties of Ni and Co-ferrite nanoparticles. *Journal of Magnetism and Magnetic Materials* **2019**, *473*, 228-235, https://doi.org/10.1016/j.jmmm.2018.10.023.
20. Maddaiah, M.; Kumar, A.G.; Obulapathi, L.; Sarmash, T.S.;Naidu, K.C.B.; Rani, D.J.; Rao, T.S. Synthesis and characterization of strontium doped zinc manganese titanate ceramics.*Digest Journal of Nanomaterials and Biostructures***2015**, *10,* 155-159.
21. Chandra. B.N.K. Microwave Processed NiMgZn Ferrites for Electromagnetic Interference Shielding Applications. *IEEE Transactions on Magnetics* **2017**, *53*, https://doi.org/10.1109/TMAG.2016.2625773.
22. Naidu, C.B.K.; Madhuri, W. Effect of Nonmagnetic Zn2+ Cations on Initial Permeability of Microwave-Treated NiMg Ferrites. *International Journal of Applied Ceramic Technology* **2016**, *13*, 1090-1095, https://doi.org/10.1111/ijac.12571.
23. Vidya Sagar T.; Subba Rao T.; Chandra Babu Naidu K.; Effect of calcination temperature on optical, magnetic and dielectric properties of Sol-Gel synthesized $Ni_{0.2}Mg_{0.8-x}Zn_xFe_2O_4$ (x = 0.0–0.8). *Ceramic International* **2020**, https://doi.org/10.1016/j.ceramint.2020.01.178
24. Ramaprasad, T.; Kumar, R.J.; Naresh, U.; Prakash, M.; Kothandan, D.; Naidu, K.C.B. Effect of pH Value on Structural and Magnetic Properties of $CuFe_2O_4$ Nanoparticles Synthesized by Low Temperature Hydrothermal Technique.*Materials Research Express***2018**,*5*, https://doi.org/10.1088/2053-1591/aad860
25. Sivakumar, D.; Naidu, K.C.B.; Nazeer, K.P.; Rafi, M.M.; Rameshkumar, G.; Sathyaseelan, B.; Killivalavan, G.; Begam, A.A. Structural Characterization and dielectric properties of Superparamagnetic Iron oxide nanoparticles.*Journal of the Korean Ceramic Society***2018**, 55, 1-9.
26. Sivakumar, D.; Naidu, K.C.B.; Rafi, M.M.; Sathyaseelan, B.; Nazeer, K.P.; Begam, A.A. Structural and dielectric properties of superparamagnetic iron oxide nanoparticles (SPIONS) stabilized by sugar solutions.*Materials Science-Poland***2018**, *36,* 123-133, https://doi.org/10.1515/msp-2018-0017
27. Liu, Y.; Drew, M.; Liu, Y. Preparation and magnetic properties of barium ferrites substitutedwith manganese, cobalt, and tin. *Journal of Magnetism and Magnetic Materials* **2010**, *323*, 945–953, https://doi.org/10.1016/j.jmmm.2010.11.075.
28. Dai, Y.; Lan, Z.; Wu, C.; Yang, C.; Yu, Z.; Guo, R.; Wang, W.; Chen, C.; Liu, X.; Jiang, X.; Sun, K. Tailoring magnetic properties of Al-substituted M-type strontium hexaferrites. *Applied Physics A* **2018**, *124*, https://doi.org/10.1007/s00339-018-2224-y.
29. Haq, A.; Anis-ur-Rehman, M. Effect of Pb on structural and magnetic properties of Ba-hexaferrite.*Physica B***2012,** 407, 822-826, https://doi.org/10.1016/j.physb.2011.11.038
30. Li, W.; Qiao, X.; Li, M.; Liu, T.; Peng, H.-X. La and Co substituted M-type barium ferrites processed by sol–gel combustion synthesis. *Materials Research Bulletin* **2013**, *48*, 4449-4453, https://doi.org/10.1016/j.materresbull.2013.07.044.
31. Rafiq, M.A.; Waqar, M.; Muhammad, Q.K.; Waleed, M.; Saleem, M.; Anwar, M.S. Conduction mechanism and magnetic behavior of Cu doped barium hexaferrite ceramics. *Journal of Materials Science: Materials in Electronics* **2018**, *29*, 5134-5142, https://doi.org/10.1007/s10854-017-8477-y.
32. Geiler, A.; He, Y.; Yoon, S.; Yang, A.; Chen, Y.; Harris, V.; Vittoria, C. Epitaxial growth of PbFe12O19 thin films by alternating target laser ablation deposition of Fe2O3 and PbO. *Journal of Applied Physics - J APPL PHYS* **2007**, *101*, https://doi.org/10.1063/1.2710222.
33. Ahmad, M.; Kriegisch, M.; Kubel, F.; Rana, M. Magnetic and microwave attenuation behavior of Al-substituted Co2W hexaferrites synthesized by sol-gel autocombustion process. *Current Applied Physics* **2012**, *12*, 1413-1420, https://doi.org/10.1016/j.cap.2012.02.038.
34. Luo, H.; Rai, B.; Mishra, S.; Nguyen, V.; Liu, J.P. Physical and magnetic properties of highly aluminum doped strontium ferrite nanoparticles prepared by auto-combustion route. *Journal of Magnetism and Magnetic Materials* **2012**, *324*, 2602-2608, https://doi.org/10.1016/j.jmmm.2012.02.106.
35. Mishra, D.; Anand, S.; Panda, R.; Das, R. X-ray diffraction studies on aluminum-substituted barium hexaferrite. *Materials Letters - MATER LETT* **2004**, *58*, 1147-1153, https://doi.org/10.1016/j.matlet.2003.08.027.

6. ACKNOWLEDGEMENTS

This work was supported by funding from University Grants Commission, New Delhi, India, under the Departmental Research Support (DRS) - Special Assistance Programme (SAP)-I.